The electronic structure and chemical bonding of aluminum acetylide: Al_2C_2 and $Al_2C_2^-$: An experimental and theoretical investigation

Nathan A. Cannon and Alexander I. Boldyrev[a)]
Department of Chemistry and Biochemistry, Utah State University, Logan, Utah 84322-0300

Xi Li and Lai-Sheng Wang[b)]
Department of Physics, Washington State University, and W. R. Wiley Environmental Molecular Sciences Laboratory, Pacific Northwest National Laboratory, MS K8-88, P. O. Box 999, Richland, Washington 99352

(Received 11 April 2000; accepted 19 May 2000)

We have investigated the electronic structure and chemical bonding of Al_2C_2 and $Al_2C_2^-$ both experimentally and theoretically. Photoelectron spectra of $Al_2C_2^-$ were obtained at several photon energies. Two anionic isomers were observed: one with a very sharp ground state feature and a low vertical electron binding energy (0.71 eV) and another with a very broad ground state feature with a much higher vertical electron binding energy (1.58 eV). Theoretical calculations were performed at various levels of theory for both the anion and the neutral. We found two isomers with relatively close energies for the anion: a quasilinear acetylide species and a planar-bridged D_{2h} structure. However, only one stable isomer was found for the neutral, which has the acetylide structure. Adiabatic and vertical detachment energies were also calculated for the two anionic isomers and were used to interpret and assign the experimental spectra. We found that the sharp 0.71 eV feature was from the acetylide isomer, whereas the broad 1.58 eV feature was from the D_{2h} isomer. The excellent agreement between the calculated and experimental electron affinities and excitation energies lends considerable credence for the assignments of the two anionic isomers. The structures and bonding of the acetylide neutral and anion and the D_{2h} anion are discussed. © *2000 American Institute of Physics.* [S0021-9606(00)30831-5]

I. INTRODUCTION

Carbon–aluminum mixed clusters often demonstrate the preference of nonclassical structures.[1–4] Among such structures we can cite the recent discovery of tetracoordinate planar carbon in CAl_4^-, CAl_5, and CAl_5^-,[1,2] as well as π coordination of Al in AlC_2[3,4] and AlC_2^-.[4] Understanding of small Al–C clusters may not only reveal novel chemical structures and bonding, but it may also provide insight into bulk carbide materials. On the bases of the π coordination of Al in $AlC_2(AlC_2^-)$ and the planar-bridged structure of Li_2C_2,[5–8] one would expect that both Al_2C_2 and $Al_2C_2^-$ should have the planar-bridged (D_{2h} rhombus) structures. However, our current knowledge about even the very small carbon–aluminum species is too limited to allow such predictions. As we show in the current paper, the carbon–aluminum systems continue to reveal surprises. We have found that the Al_2C_2 molecule has a quasilinear (acetylide) structure, while the $Al_2C_2^-$ anion has both the acetylenic and the planar-bridged structures.

Photoelectron spectroscopy (PES) of size-selected anions combined with a laser vaporization cluster source has been proven to be a powerful experimental technique to study the electronic structure of a wide range of novel molecular and cluster species. In the present study, we combine PES and an extensive *ab initio* investigation on Al_2C_2 and $Al_2C_2^-$, neither of which has been reported previously. The PES spectra of $Al_2C_2^-$ contain numerous features, corresponding to detachment to the ground and excited states of neutral Al_2C_2. In particular, the current experiment revealed the existence of two anionic isomers, with vertical detachment energies (VDEs) of 0.71 and 1.58 eV, respectively. *Ab initio* calculations were performed for both the anion and the neutral. Indeed, two isomers were found theoretically for the $Al_2C_2^-$ anion (a quasilinear acetylide and a planar-bridged species), whereas a single acetylide species was found for neutral Al_2C_2. The theoretical calculations predicted a lower VDE for the acetylide isomer and a higher VDE for the rhombus species, consistent with the experimental observations. The calculated electron affinities and neutral excitation energies are in good agreement with the experiment, thus allowing us to characterize the geometrical and electronic structures of the Al_2C_2 molecule and its anions.

II. EXPERIMENT

The experiments were performed with a magnetic-bottle time-of-flight PES apparatus equipped with a laser vaporization cluster source. Details of the experiment have been described previously.[9,10] Briefly, the $Al_2C_2^-$ anions were produced by laser vaporization of a graphite/aluminum mixed target with a pure helium carrier gas. The clusters formed from the laser vaporization source were entrained in the He carrier gas and underwent a supersonic expansion. The anion

a)Electronic mail: boldyrev@cc.usu.edu
b)Electronic mail: ls.wang@pnl.gov

species in the beam were extracted perpendicularly into a time-of-flight mass spectrometer. Various mixed clusters composed of $Al_xC_y^-$ were formed from the source, predominantly with $y=1$ and 2. The $Al_2C_2^-$ anions were selected and decelerated before photodetachment by a laser beam. For the current experiment, both a Nd:YAG laser (532, 355, and 266 nm) and an ArF excimer laser (193 nm) were used for photodetachment. The energy scales were calibrated with the known spectra of Cu^- and the electron kinetic energy resolution of the apparatus was better than 30 meV for 1 eV electrons.

III. COMPUTATIONAL METHODS

We first optimized the geometries of Al_2C_2 and $Al_2C_2^-$, employing analytical gradients with polarized split-valence basis sets (6-311+G*)[11–13] with a hybrid method, which includes a mixture of Hartree–Fock exchange with density functional exchange-correlation (B3LYP) potential.[14–16] The lowest energy structures thereby identified were refined at the second-order Møller-Plesset perturbation theory (MP2(full))[17] and coupled-cluster single, double, and triple approximate excitations (CCSD(T))[18–20] levels of theory. Finally, the energies of the lowest structures were refined even further using the CCSD(T) levels of theory and 6-311 +G(2df) basis sets.

VDEs from the lowest-energy structures of $Al_2C_2^-$ were calculated using the unrestricted outer valence Green function (UOVGF) method[21–25] incorporated in GAUSSIAN-98. For the lowest states in every symmetry we also calculated VDEs using the CCSD(T)/6-311+G(2df) level of theory. As we will show in Sec. V, two isomers were found for $Al_2C_2^-$ and both have doublet ground states. Thus, both triplet and singlet excited states of the neutrals can be reached in the photodetachment processes. We stress hereby that we were able to calculate the VDEs only to the triplet excited states using the UOVGF and CCSD(T) methods, because the electron detachment processes leading to the corresponding singlet excited states would require multiconfiguration reference wave functions, which are not available in the current theoretical methods employed. For the lowest detachment channel the final singlet state is essentially single configuration and therefore we were able to calculate the VDE using the UOVGF and CCSD(T) methods. The UOVGF calculations assure that we did not miss any one-electron detachment processes, because they allow us to calculate electron detachment energies from all orbitals (except the singlet excited states). The core electrons were kept frozen [except MP2(full)] in treating the electron correlation at the UOVGF and CCSD(T) levels of theory. All calculations were performed using the GAUSSIAN-98 program.[26]

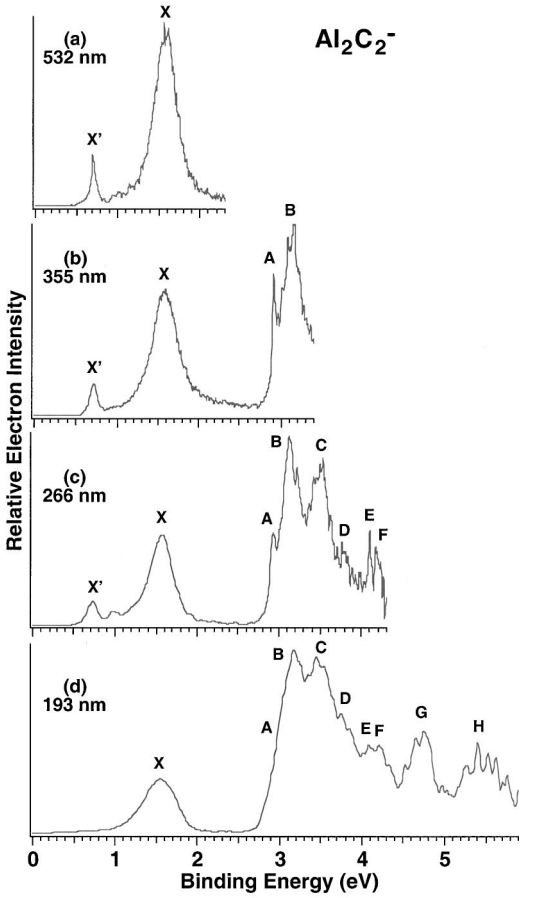

FIG. 1. Photoelectron spectra of $Al_2C_2^-$ at 532 nm (a), 355 nm (b), 266 nm (c), and 193 nm (d).

IV. EXPERIMENTAL RESULTS

The photoelectron spectra of $Al_2C_2^-$ are shown in Fig. 1 at the four detachment photon energies. The 532 nm spectrum [Fig. 1(a)] shows a weak and sharp peak at 0.71 eV, labeled X' and an intense broad feature (X) with a VDE of 1.58 eV. At 355 nm [Fig. 1(b)], at least two new features were observed at higher binding energies, a sharp feature (A) with a VDE of 2.91 eV and a broad feature (B) with a VDE of 3.12 eV. The B feature contains fine structures either due to vibrational excitations or additional electronic transitions. At 266 nm [Fig. 1(c)], several more features were observed at higher binding energies and the spectral features became rather congested. We tentatively identified four additional features, $C-F$, as shown in Fig. 1(c). More features (G and H) were further revealed in the 193 nm spectrum [Fig. 1(d)] beyond the 266 nm spectral range. The G and H features were broad and may contain more electronic transitions. At

TABLE I. The ADEs and VDEs (eV) of the observed photodetachment features from $Al_2C_2^-$.

	X'	X	A	B	C	D	E	F	G	H
ADE[a]	0.64 (5)	⋯	2.91 (3)	⋯	⋯	⋯	⋯	⋯	⋯	⋯
VDE[a]	0.71 (2)	1.58 (5)	2.91 (3)	3.12 (6)	3.50 (9)	3.8 (1)	4.10 (5)	4.20 (5)	4.7	5.5

[a]The number in parentheses represents the uncertainty of the last digit.

TABLE II. Calculated molecular properties of the most stable Al_2C_2 structures.

Al_2C_2 ($D_{\infty h}$, $^1\Sigma_g^+$)	Al_2C_2 ($D_{\infty h}$, $^1\Sigma_g^+$)	Al_2C_2 ($D_{\infty h}$, $^1\Sigma_g^+$)
B3LYP/6-311+G*	MP2(full)/6-311+G*	CCSD(T)/6-311+G*
$E_{tot}=-561.049\ 810$ a.u.	$E_{tot}=-560.154\ 371$ a.u.	$E_{tot}=-559.915\ 257$ a.u.
$\Delta E_{tot}=0.0$ kcal/mol	$\Delta E_{tot}=0.05$ kcal/mol	$\Delta E_{tot}=0.11$ kcal/mol
R(C–C)=1.238 Å	R(C–C)=1.258 Å	R(C–C)=1.254 Å
R(C–Al)=1.985 Å	R(C–Al)=1.977 Å	R(C–Al)=1.979 Å
$\omega_1(\sigma_g)=2074\ cm^{-1}$	$\omega_1(\sigma_g)=1954\ cm^{-1}$	$\omega_1(\sigma_g)=2003\ cm^{-1}$
$\omega_2(\sigma_g)=349\ cm^{-1}$	$\omega_2(\sigma_g)=357\ cm^{-1}$	$\omega_2(\sigma_g)=357\ cm^{-1}$
$\omega_3(\sigma_u)=606\ cm^{-1}$	$\omega_3(\sigma_u)=626\ cm^{-1}$	$\omega_3(\sigma_u)=626\ cm^{-1}$
$\omega_4(\pi_g)=93\ cm^{-1}$	$\omega_4(\pi_g)=178\ i\ cm^{-1}$	$\omega_4(\pi_g)=237\ i\ cm^{-1}$
$\omega_5(\pi_u)=60\ cm^{-1}$	$\omega_5(\pi_u)=55\ cm^{-1}$	$\omega_5(\pi_u)=45\ cm^{-1}$
⋯	Al_2C_2 (C_{2h}, ^1A_g)	Al_2C_2 (C_{2h}, ^1A_g)
⋯	MP2(full)/6-311+G*	CCSD(T)/6-311+G*
⋯	$E_{tot}=-560.154\ 446$ a.u.	$E_{tot}=-559.915\ 428$ a.u.
⋯	$\Delta E_{tot}=0.0$ kcal/mol	$\Delta E_{tot}=0.0$ kcal/mol
⋯	R(C–C)=1.258 Å	R(C–C)=1.255 Å
⋯	R(C–Al)=1.978 Å	R(C–Al)=1.980 Å
⋯	<AlCC=172.6°	<AlCC=171.3°
⋯	$\omega_1(a_g)=1951\ cm^{-1}$	$\omega_1(a_g)=1998\ cm^{-1}$
⋯	$\omega_2(a_g)=363\ cm^{-1}$	$\omega_2(a_g)=367\ cm^{-1}$
⋯	$\omega_3(a_g)=176\ cm^{-1}$	$\omega_3(a_g)=209\ cm^{-1}$
⋯	$\omega_4(a_u)=58\ cm^{-1}$	$\omega_4(a_u)=53\ cm^{-1}$
⋯	$\omega_5(b_u)=626\ cm^{-1}$	$\omega_5(b_u)=626\ cm^{-1}$
⋯	$\omega_6(b_u)=64\ cm^{-1}$	$\omega_6(b_u)=66\ cm^{-1}$

193 nm, the X' feature became rather weak and was hardly visible, suggesting that it may be due to a different isomer or an electronically excited $Al_2C_2^-$ anion. The obtained VDEs and ADEs (adiabatic detachment energies) for the various features are summarized in Table I.

As we will show below from the theoretical investigations, there are indeed two anionic isomers fairly close in energy: an acetylide quasilinear species and a rhombus isomer. The acetylide species has a lower VDE, corresponding to the X' feature, whereas the rhombus isomer has a fairly high VDE corresponding to the X feature.

V. THEORETICAL RESULTS

A. Structures of Al_2C_2

We started geometry optimizations of Al_2C_2 with a linear $D_{\infty h}$ species ($^1\Sigma_g^+, 1\sigma_g^2 1\sigma_u^2 2\sigma_g^2 1\pi_u^4 2\sigma_u^2 3\sigma_g^2 1\pi_g^0$) and a planar-bridged D_{2h} species

$$(^1A_g, 1a_g^2 1b_{1u}^2 1b_{2u}^2 2a_g^2 1b_{3u}^2 3a_g^2 2b_{1u}^2 1b_{3g}^0)$$

using B3LYP/6-311+G* level of theory. The linear structure was found to be a minimum (Table II), but the D_{2h} structure was found to be a third order saddle point and 26.7 kcal/mol higher in energy (Table III). Geometry optimization was then performed upon lowering the symmetry from D_{2h} to C_{2v}. First, we allowed out-of-plane deformation leading to a butterfly-type bridged C_{2v}–I structure (Table III), which was found to be a second order saddle point. Then we allowed in-plane deformation leading to the vinylidene C_{2v}–II structure (Table III), which was found to be a first order saddle point. Both structures are substantially higher in energy than the linear structure with relative energies being 26.5 kcal/mol (C_{2v}–I) and 19.6 kcal/mol (C_{2v}–II) higher.

TABLE III. Calculated molecular properties of the alternative Al_2C_2 structures.

Al_2C_2 (D_{2h}, ^1A_g)	Al_2C_2 (D_{2h}, ^1A_g)	Al_2C_2 (D_{2h}, ^1A_g)
B3LYP/6-311+G*	MP2(full)/6-311+G*	CCSD(T)/6-311+G*
$E_{tot}=-561.007\ 217$ a.u.	$E_{tot}=-560.115\ 954$ a.u.	$E_{tot}=-559.876\ 312$ a.u.
$\Delta E_{tot}=26.7$ kcal/mol	$\Delta E_{tot}=24.1$ kcal/mol	$\Delta E_{tot}=24.5$ kcal/mol
R(C–C)=1.257 Å	R(C–C)=1.279 Å	R(C–C)=1.277 Å
R(C–Al)=2.213 Å	R(C–Al)=2.192 Å	R(C–Al)=2.193 Å
$\omega_1(a_g)=1864\ cm^{-1}$	$\omega_1(a_g)=1750\ cm^{-1}$	$\omega_1(a_g)=1783\ cm^{-1}$
$\omega_2(a_g)=301\ cm^{-1}$	$\omega_2(a_g)=317\ cm^{-1}$	$\omega_2(a_g)=316\ cm^{-1}$
$\omega_3(b_{3g})=486\ i\ cm^{-1}$	$\omega_3(b_{3g})=474\ i\ cm^{-1}$	$\omega_3(b_{3g})=474\ i\ cm^{-1}$
$\omega_4(b_{1u})=466\ cm^{-1}$	$\omega_4(b_{1u})=493\ cm^{-1}$	$\omega_4(b_{1u})=500\ cm^{-1}$
$\omega_5(b_{2u})=116\ i\ cm^{-1}$	$\omega_5(b_{2u})=73\ i\ cm^{-1}$	$\omega_5(b_{2u})=101\ i\ cm^{-1}$
$\omega_6(b_{3u})=46\ i\ cm^{-1}$	$\omega_6(b_{3u})=62\ i\ cm^{-1}$	$\omega_6(b_{3u})=68\ i\ cm^{-1}$
Al_2C_2 ($C_{2v,I}$, $^1A_1$)	Al_2C_2 ($C_{2v,I}$, $^1A_1$)[a]	Al_2C_2 ($C_{2v,I}$, $^1A_1$)[b]
B3LYP/6-311+G*	MP2(full)/6-311+G*	CCSD(T)/6-311+G*
$E_{tot}=-561.007\ 632$ a.u.	$E_{tot}=-560.116\ 772$ a.u.	$E_{tot}=-559.877\ 370$ a.u.
$\Delta E_{tot}=26.5$ kcal/mol	$\Delta E_{tot}=23.6$ kcal/mol	$\Delta E_{tot}=23.9$ kcal/mol
R(C–C)=1.257 Å	R(C–C)=1.279 Å	R(C–C)=1.277 Å
R(C–Al)=2.214 Å	R(C–Al)=2.195 Å	R(C–Al)=2.198 Å
<AlCAl=133.3°	<AlCAl=130.9°	<AlCAl=129.5°
$\omega_1(a_1)=1865\ cm^{-1}$	$\omega_1(a_1)=1754\ cm^{-1}$	$\omega_1(a_1)=1787\ cm^{-1}$
$\omega_2(a_1)=328\ cm^{-1}$	$\omega_2(a_1)=348\ cm^{-1}$	$\omega_2(a_1)=349\ cm^{-1}$
$\omega_3(a_1)=55\ cm^{-1}$	$\omega_3(a_1)=69\ cm^{-1}$	$\omega_3(a_1)=72\ cm^{-1}$
$\omega_4(a_2)=454\ i\ cm^{-1}$	$\omega_4(a_2)=440\ i\ cm^{-1}$	$\omega_4(a_2)=436\ i\ cm^{-1}$
$\omega_5(b_1)=454\ cm^{-1}$	$\omega_5(b_1)=476\ cm^{-1}$	$\omega_5(b_1)=479\ cm^{-1}$
$\omega_6(b_2)=140\ i\ cm^{-1}$	$\omega_6(b_2)=94\ i\ cm^{-1}$	$\omega_6(b_2)=133\ i\ cm^{-1}$
Al_2C_2 ($C_{2v,II}$, $^1A_1$)	Al_2C_2 ($C_{2v,II}$, $^1A_1$)	Al_2C_2 ($C_{2v,II}$, $^1A_1$)
B3LYP/6-311+G*	MP2(full)/6-311+G*	CCSD(T)/6-311+G*
$E_{tot}=-561.018\ 576$ a.u.	$E_{tot}=-560.120\ 581$ a.u.	$E_{tot}=-559.884\ 978$ a.u.
$\Delta E_{tot}=19.6$ kcal/mol	$\Delta E_{tot}=21.3$ kcal/mol	$\Delta E_{tot}=19.1$ kcal/mol
R(C–C)=1.273 Å	R(C–C)=1.284 Å	R(C–C)=1.289 Å
R(C–Al)=2.015 Å	R(C–Al)=2.010 Å	R(C–Al)=2.007 Å
<AlCC=110.5°	<AlCC=106.6°	<AlCC=109.7°
$\omega_1(a_1)=1799\ cm^{-1}$	$\omega_1(a_1)=1770\ cm^{-1}$	$\omega_1(a_1)=1748\ cm^{-1}$
$\omega_2(a_1)=384\ cm^{-1}$	$\omega_2(a_1)=379\ cm^{-1}$	$\omega_2(a_1)=391\ cm^{-1}$
$\omega_3(a_1)=110\ cm^{-1}$	$\omega_3(a_1)=91\ cm^{-1}$	$\omega_3(a_1)=102\ cm^{-1}$
$\omega_4(b_1)=156\ cm^{-1}$	$\omega_4(b_1)=108\ i\ cm^{-1}$	$\omega_4(b_1)=83\ i\ cm^{-1}$
$\omega_5(b_2)=645\ cm^{-1}$	$\omega_5(b_2)=662\ cm^{-1}$	$\omega_5(b_2)=674\ cm^{-1}$
$\omega_6(b_2)=33\ i\ cm^{-1}$	$\omega_6(b_2)=161\ i\ cm^{-1}$	$\omega_6(b_2)=117\ i\ cm^{-1}$

[a]Optimization of this structure along the out-of-plane imaginary frequency mode leads to the slightly nonplanar structure: $C_s(^1A')$, $E_{tot}=-560.120\ 676$ a.u., R(C–C)=1.284 Å, R(C–Al)=2.012 Å, <AlCC=105.7°, <AlCAl=145.4°, $\omega_1(a')=1767\ cm^{-1}$, $\omega_2(a')=383\ cm^{-1}$, $\omega_3(a')=111\ cm^{-1}$, $\omega_4(a')=91\ cm^{-1}$, $\omega_5(a'')=655\ cm^{-1}$, $\omega_6(a'')=159\ i\ cm^{-1}$.

[b]Optimization of this structure along the out-of-plane imaginary frequency mode leads to the slightly nonplanar structure: $C_s(^1A')$, $E_{tot}=-559.885\ 005$ a.u., R(C–C)=1.289 Å, R(C–Al)=2.008 Å, <AlCC=109.2°, <AlCAl=140.2°, $\omega_1(a')=1748\ cm^{-1}$, $\omega_2(a')=393\ cm^{-1}$, $\omega_3(a')=103\ cm^{-1}$, $\omega_4(a')=100\ cm^{-1}$, $\omega_5(a'')=670\ cm^{-1}$, $\omega_6(a'')=114\ i\ cm^{-1}$.

Upon further refinement at the MP2(full)/6-311+G* level of theory, the linear structure was found to be a second order saddle point (Table II). Following its (degenerate) imaginary-frequency distortion, further geometry optimization led to a quasilinear

$$C_{2h}\,(^1A_g, 1a_g^2 1b_u^2 2a_g^2 1a_u^2 2b_u^2 3b_u^2 3a_g^2 1b_g^0)$$

structure (Table II), which is the global minimum at the MP2(full)/6-311+G* level of theory. The linear structure

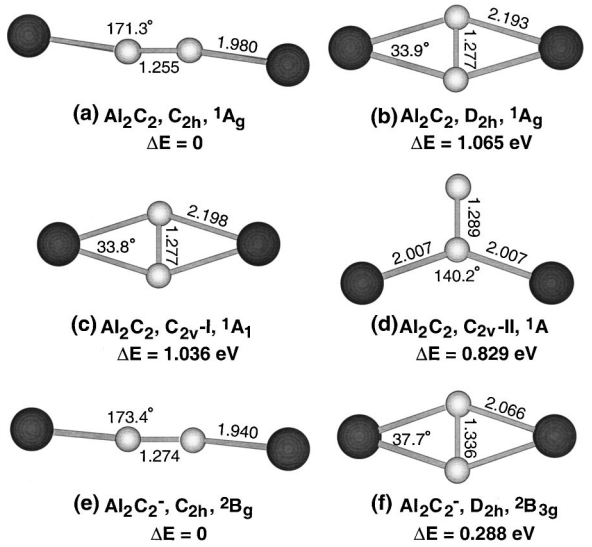

FIG. 2. Optimized Al_2C_2 and $Al_2C_2^-$ structures at the CCSD(T)/6-311+G* level of theory (see Tables II–IV for parameters).

was found to be just 0.047 kcal/mol higher in energy. Further examination of this structure at the CCSD(T) level of theory revealed the same results with the C_{2h} structure being 0.107 kcal/mol lower in energy than the linear one [Table II and Fig. 2(a)]. Therefore, when the zero-point energy (ZPE) corrections are taken into account (ΔZPE=0.349 kcal/mol) the vibrationally averaged structure is essentially linear.

Results are very similar for the D_{2h} [Fig. 2(b)], $C_{2v}-I$ [Fig. 2(c)], and $C_{2v}-II$ [Fig. 2(d)] structures at the MP2(full) and CCSD(T) level of theory. When the symmetry of the $C_{2v}-II$ structure was lowered during geometry optimization, we found that the true first order saddle point corresponds to the C_s ($^1A'$) structure. However, the deviation from planarity for the C_s ($^1A'$) structure is very small. The barrier of planarization was found to be just 0.017 kcal/mol, which is smaller than the difference in the ZPE corrections (0.141 kcal/mol) for the $C_{2v}-II$ and the C_s structures. Therefore, the vibrationally averaged C_s structure actually has the C_{2v} symmetry [Fig. 2(d) and Table III]. Based on the above results, we conclude that Al_2C_2 is quasilinear [Fig. 2(a)] at the potential energy surface level, but is effectively a linear acetylide after ZPE corrections are taken into account.

B. Structure of $Al_2C_2^-$

Similar to the neutral, we first optimized geometries of a linear $(D_{\infty h},{}^2\Pi_g,1\sigma_g^2 1\sigma_u^2 2\sigma_g^2 1\pi_u^4 2\sigma_u^2 3\sigma_g^2 1\pi_g^1)$ and a planar-bridged

$$(D_{2h},{}^2B_{3g},1a_g^2 1b_{1u}^2 1b_{2u}^2 2a_g^2 1b_{3u}^2 3a_g^2 2b_{1u}^2 1b_{3g}^1)$$

structure for $Al_2C_2^-$ using B3LYP/6-311+G* level of theory. Both structures were found to be minima with the linear structure being more stable by 14.1 kcal/mol (Table IV). The doubly degenerate vibrational states of the $D_{\infty h}$ structure are split due to single occupation of the doubly degenerate $1\pi_g$ molecular orbital (MO) ($^2\Pi_g$). To regain the degeneracy one may use one of several averaging schemes. In the simplest approach, we got $\omega_4(\pi_g)=236\,\mathrm{cm}^{-1}$ and $\omega_5(\pi_u)=88\,\mathrm{cm}^{-1}$. A quartet linear structure $(D_{\infty h},{}^4\Sigma_g^-,1\sigma_g^2 1\sigma_u^2 2\sigma_g^2 1\pi_u^4 2\sigma_u^2 3\sigma_g^1 1\pi_g^2)$ was also optimized. It was found to be a minimum, but is 46.0 kcal/mol higher than the linear doublet state. Thus it was excluded from further examination. The vinylidene-type structure collapsed into the rhombus structure upon geometry optimization.

TABLE IV. Calculated molecular properties of the $Al_2C_2^-$ structures.

$Al_2C_2^-$ ($D_{\infty h}$,$^2\Pi_g$)	$Al_2C_2^-$ ($D_{\infty h}$,$^2\Pi_g$)	$Al_2C_2^-$ ($D_{\infty h}$,$^2\Pi_g$)[b]
B3LYP/6-311+G*	MP2(full)/6-311+G*	CCSD(T)/6-311+G*
$E_{tot}=-561.083\,800$ a.u.	$E_{tot}=-560.168\,787$ a.u.	$E_{tot}=-559.929\,767$ a.u.
$\Delta E_{tot}=0.0$ kcal/mol	$\Delta E_{tot}=0.0$ kcal/mol	$\Delta E_{tot}=0.044$ kcal/mol
R(C–C)=1.255 Å	R(C–C)=1.274 Å	R(C–C)=1.273 Å
R(C–Al)=1.943 Å	R(C–Al)=1.934 Å	R(C–Al)=1.939 Å
$\omega_1(\sigma_g)=1920\,\mathrm{cm}^{-1}$	$\omega_1(\sigma_g)=1851\,\mathrm{cm}^{-1}$	⋯
$\omega_2(\sigma_g)=358\,\mathrm{cm}^{-1}$	$\omega_2(\sigma_g)=370\,\mathrm{cm}^{-1}$	⋯
$\omega_3(\sigma_u)=615\,\mathrm{cm}^{-1}$	$\omega_3(\sigma_u)=(3693\,\mathrm{cm}^{-1})$[a]	⋯
$\omega_4(\pi_g)=274\,\mathrm{cm}^{-1}$	$\omega_4(\pi_g)=102\,\mathrm{cm}^{-1}$	⋯
$=197\,\mathrm{cm}^{-1}$	$=62\,i\,\mathrm{cm}^{-1}$	⋯
$\omega_5(\pi_u)=99\,\mathrm{cm}^{-1}$	$\omega_5(\pi_u)=88\,\mathrm{cm}^{-1}$	⋯
$=77\,\mathrm{cm}^{-1}$	$=69\,\mathrm{cm}^{-1}$	⋯
⋯	$Al_2C_2^-$ (C_{2h},^2B_g)	$Al_2C_2^-$ (C_{2h},^2B_g)[b]
⋯	MP2(full)/6-311+G*	CCSD(T)/6-311+G*
⋯	$E_{tot}=-560.168\,787$ a.u.	$E_{tot}=-559.929\,837$ a.u.
⋯	$\Delta E_{tot}=0.0$ kcal/mol	$\Delta E_{tot}=0.0$ kcal/mol
⋯	R(C–C)=1.274 Å	R(C–C)=1.274 Å
⋯	R(C–Al)=1.934 Å	R(C–Al)=1.940 Å
⋯	<AlCC=178.5	<AlCC=173.7
⋯	$\omega_1(a_g)=1850\,\mathrm{cm}^{-1}$	⋯
⋯	$\omega_2(a_g)=370\,\mathrm{cm}^{-1}$	⋯
⋯	$\omega_3(a_g)=80\,\mathrm{cm}^{-1}$	⋯
⋯	$\omega_4(a_u)=88\,\mathrm{cm}^{-1}$	⋯
⋯	$\omega_5(b_u)=(3696\,\mathrm{cm}^{-1})$[a]	⋯
⋯	$\omega_6(b_u)=70\,\mathrm{cm}^{-1}$	⋯
$Al_2C_2^-$ (D_{2h},$^2B_{3g}$)	$Al_2C_2^-$ (D_{2h},$^2B_{3g}$)	$Al_2C_2^-$ (D_{2h},$^2B_{3g}$)
B3LYP/6-311+G*	MP2(full)/6-311+G*	CCSD(T)/6-311+G*
$E_{tot}=-561.061\,370$ a.u.	$E_{tot}=-560.160\,595$ a.u.	$E_{tot}=-559.919\,184$ a.u.
$\Delta E_{tot}=14.1$ kcal/mol	$\Delta E_{tot}=5.1$ kcal/mol	$\Delta E_{tot}=6.64$ kcal/mol
R(C–C)=1.310 Å	R(C–C)=1.335 Å	R(C–C)=1.336 Å
R(C–Al)=2.079 Å	R(C–Al)=2.064 Å	R(C–Al)=2.066 Å
$\omega_1(a_g)=1543\,\mathrm{cm}^{-1}$	$\omega_1(a_g)=1471\,\mathrm{cm}^{-1}$	$\omega_1(a_g)=1464\,\mathrm{cm}^{-1}$
$\omega_2(a_g)=334\,\mathrm{cm}^{-1}$	$\omega_2(a_g)=357\,\mathrm{cm}^{-1}$	$\omega_2(a_g)=357\,\mathrm{cm}^{-1}$
$\omega_3(b_{3g})=380\,\mathrm{cm}^{-1}$	$\omega_3(b_{3g})=431\,\mathrm{cm}^{-1}$	$\omega_3(b_{3g})=411\,\mathrm{cm}^{-1}$
$\omega_4(b_{1u})=601\,\mathrm{cm}^{-1}$	$\omega_4(b_{1u})=636\,\mathrm{cm}^{-1}$	$\omega_4(b_{1u})=637\,\mathrm{cm}^{-1}$
$\omega_5(b_{2u})=141\,\mathrm{cm}^{-1}$	$\omega_5(b_{2u})=197\,\mathrm{cm}^{-1}$	$\omega_5(b_{2u})=161\,\mathrm{cm}^{-1}$
$\omega_6(b_{3u})=94\,\mathrm{cm}^{-1}$	$\omega_6(b_{3u})=101\,\mathrm{cm}^{-1}$	$\omega_5(b_{3u})=96\,\mathrm{cm}^{-1}$

[a]This frequency experiences a symmetry broken problem.
[b]Frequencies were not calculated at this level of theory due to convergence problems during numerical evaluations of the second derivatives.

At the MP2(full)/6-311+G* level of theory, the $(D_{2h},{}^2B_{3g})$ structure was found again to be a minimum, but the $(D_{\infty h},{}^2\Pi_g)$ linear structure was found to have one imaginary frequency (Table IV). Geometry optimization using a lower symmetry led to a quasilinear $(C_{2h},{}^2B_g)$ structure. At the CCSD(T)/6-311+G* level of theory, we found that both the $(C_{2h},{}^2B_g)$ and $(D_{2h},{}^2B_{3g})$ structures are minima with the quasilinear structure [Fig. 2(e)] being the global minimum and the rhombus structure [Fig. 2(f)] being a low-lying isomer. At our highest level of theory (CCSD(T)/6-311

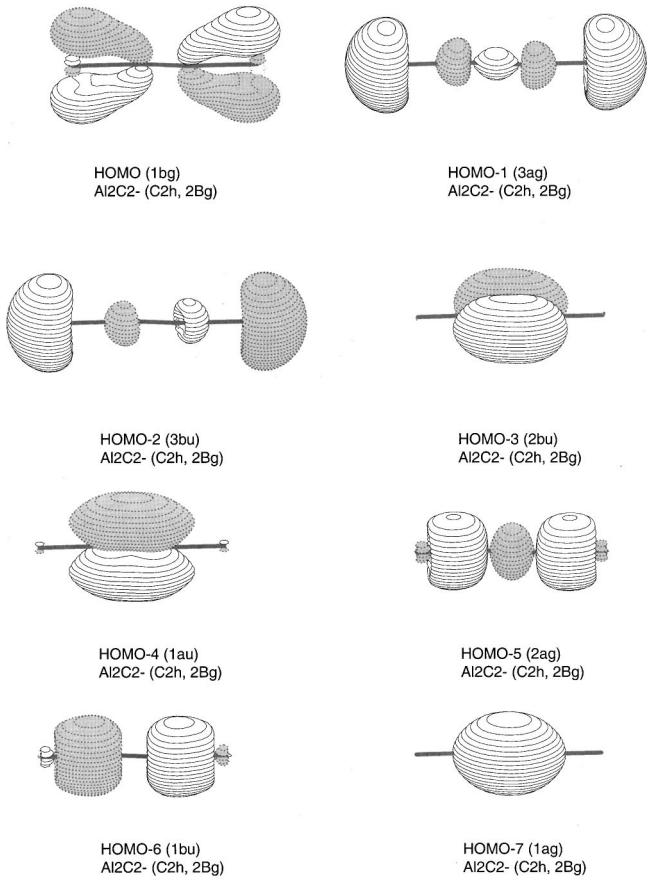

FIG. 3. Molecular orbital pictures (Ref. 27) showing the MOs of the C_{2h} $Al_2C_2^-$ structure.

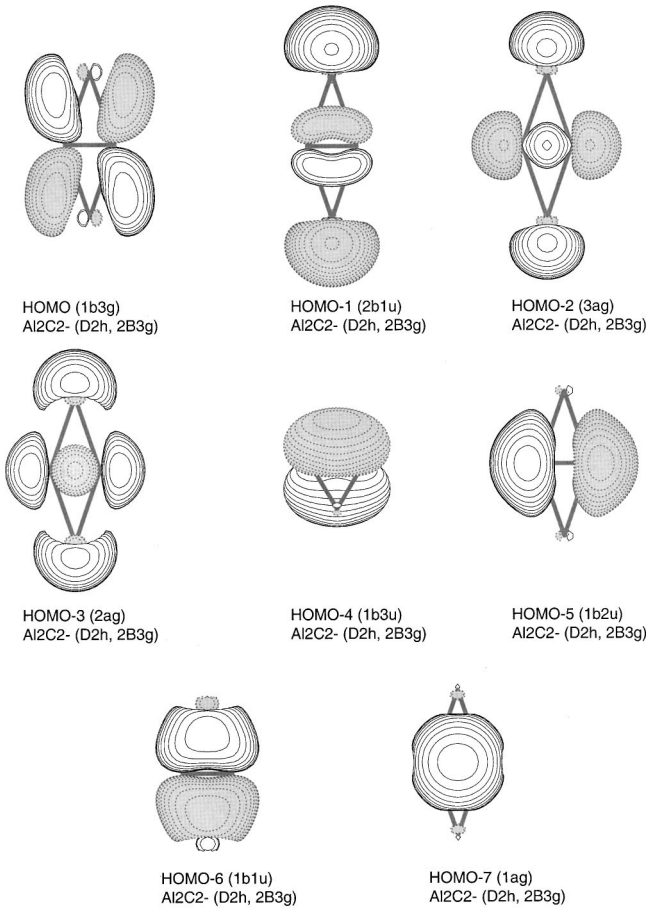

FIG. 4. Molecular orbital pictures (Ref. 27) showing the MOs of the D_{2h} $Al_2C_2^-$ structure.

+G(2df)), the $C_{2h}(^2B_g)$ quasilinear structure was found to be more stable then the $(D_{2h},^2B_{3g})$ structures by 7.2 kcal/mol. However, this energy difference based on the current *ab initio* calculations is still too small for us to make a definitive conclusion about which is the global minimum structure of $Al_2C_2^-$. In particular, one expects that the energy of the compact structure $(D_{2h},^2B_{3g})$ will be stabilized more than the $C_{2h}(^2B_g)$ quasilinear structure with larger basis sets and better treatment of correlation energies.

C. Stability of Al_2C_2 and $Al_2C_2^-$

Both the anion and neutral species were found to be quite stable. The lowest dissociation channels were found to be: $D_e=51$ kcal/mol for $Al_2C_2^-(C_{2h},^2B_g)\rightarrow AlC_2^-(C_{2v},^1A_1)+Al(^2P)$ and $D_e=97$ kcal/mol for $Al_2C_2(C_{2h},^1A_g)\rightarrow AlC_2(C_{2v},^2A_1)+Al(^2P)$ (all at the CCSD(T)/6-311+G(2df) levels of theory). Data for $AlC_2^-(C_{2v},^1A_1)$ and $AlC_2(C_{2v},^2A_1)$ were taken from Ref. 4.

D. Bonding in Al_2C_2 and $Al_2C_2^-$

The canonical order of the occupied valence MOs in the 14-valence electron quasilinear Al_2C_2 structure $C_{2h}(^1A_g)$ is $1a_g^2 1b_u^2 2a_g^2 1a_u^2 2b_u^2 3b_u^2 3a_g^2 1b_g^0$. As shown in Fig. 3,[27] the $1a_g$ orbital is the C–C σ bond; the $1b_u$ and $2a_g$ orbitals are the C–Al bonds; the $1a_u$ and $2b_u$ orbitals are the C–C π bonds; and the $3b_u$ and $3a_g$ orbitals are the Al lone pairs. The lowest unoccupied molecular orbital (LUMO, $1b_g$) has an antibonding C–C π character and a bonding C–Al π character. Therefore, the bonding picture for this quasilinear AlCCAl structure is very simple: the two Al atoms can be considered as singly charged cations (Al^+) coordinated to an acetylide dianion (C_2^{2-}) through the σ bonds with a lone pair on each Al.

The canonical order of the occupied valence MOs in the planar-bridged $D_{2h}(^1A_g)$ structure is $1a_g^2 1b_{1u}^2 1b_{2u}^2 2a_g^2 1b_{3u}^2 3a_g^2 2b_{1u}^2 1b_{3g}^0$. As shown in Fig. 4, it is more difficult to give a simple characterization of the MOs in this structure due to the mixing of bonding interactions with the lone pairs. The $1a_g$ MO can still be assigned to the C–C σ bond primarily. The $1b_{1u}$ orbital, which would be the C–C π bond in a pure C_2^{2-}, does have this character but it also has Al–C bonding contributions. The $1b_{2u}$ MO is a pure lone pair of the carbon atoms (with different signs at the two ends). The $2a_g$ MO has contributions from both the C–C bond and lone pairs of carbons and aluminums (with all signs being the same). The $1b_{3u}$ MO, which would be the second component of the C–C π bond in a pure C_2^{2-}, is of C–C π bond character with some bonding contribution from the π orbitals of Al. The $3a_g$ MO has a similar structure as the $2a_g$ MO with only one difference—the carbon lone pairs have different signs relative to the aluminum lone pairs. The $2b_{1u}$ MO is a C–C π bond with contributions from alumi-

TABLE V. Calculated and experimental electron detachment processes and binding energies of the $C_{2h}(^2B_g)$ quasilinear structure of $Al_2C_2^-$.

State	Experiment VDE (eV)	Experiment ADE (eV)	Structure, $D_{\infty h}$ Final state	Theory, VDE(eV)	Theory, ADE (eV)
X'	0.71 (2)	0.64 (5)	^1A_g	0.67[a]	0.62[a]
				0.65 (0.91)[b]	
A	2.91 (3)	⋯	^3B_g	2.85[a]	⋯
				3.28 (0.78)[b]	
	⋯	⋯	^3A_u	3.01[a]	⋯
				3.67 (0.74)[b]	
	⋯	⋯	^3B_u	4.56[a]	⋯
				4.71 (0.84)[b]	
	⋯	⋯	^3A_u	5.01 (0.84)[b]	⋯

[a]At the CCSD(T)/6-311+G(2df) level of theory using CCSD(T)/6-311+G* geometry.
[b]At the UOVGF/6-311+G(2df) level of theory using CCSD(T)/6-311+G* geometry. Pole strength is given in parentheses.

TABLE VI. Calculated and experimental electron detachment processes and binding energies of the $D_{2h}(^2B_{3g})$ rhombus structure of $Al_2C_2^-$.

State	Experiment VDE (eV)	Experiment ADE (eV)	Structure, $D_{\infty h}$ Final state	Theory, VDE (eV)	Theory, ADE (eV)
X	1.58 (5)	⋯	^1A_g	1.75[a]	0.31[a]
				1.78 (0.88)[b]	
B	3.12 (6)	⋯	$^3B_{2u}$	2.94[a]	⋯
				3.00 (0.88)[b]	
	⋯	⋯	$^3B_{3g}$	2.99[a]	⋯
				3.33 (0.87)[b]	
	⋯	⋯	$^3B_{3g}$	4.97 (0.86)[b]	⋯
	⋯	⋯	^3A_u	5.44[a]	⋯
				5.44 (0.88)[b]	

[a]At the CCSD(T)/6-311+G(2df) level of theory using CCSD(T)/6-311+G* geometry.
[b]At the UOVGF/6-311+G(2df) level of theory using CCSD(T)/6-311+G* geometry. Pole strength is given in parentheses.

num lone pairs. The LUMO ($1b_{3g}$) has an antibonding C–C π character and a bonding C–Al π character. This complicated MO picture can be reduced into a simple bonding picture, in which the two Al^+ ions are coordinated to the π bonds of C_2^{2-} in the Al_2C_2 rhombus structure with a lone pair on each Al and C.

Occupation of the LUMO ($1b_g$) of Al_2C_2 in the quasilinear anion should lead to a shortening of the Al–C bond and to elongation of the C–C bond in $Al_2C_2^-$, based on the antibonding C–C π character and bonding C–Al π character on the $1b_g$ MO (Fig. 3). That is consistent with the optimized structures of the quasilinear Al_2C_2 and $Al_2C_2^-$ (Fig. 2), even though the effect is rather modest. The reason for the small effects on the structure upon occupation of the $1b_g$ MO is due to the small overlap between the diffuse p_π orbitals of Al and the more compact p_π orbitals of C.

Occupation of the LUMO ($1b_{3g}$) in the planar-bridged isomer should lead to similar structural effects in the anion, because it also has an antibonding C–C π character and a bonding C–Al π character (Fig. 4). Indeed we found such structural changes in the optimized structures between the anion and neutral of the rhombus structure. The structural effects are much more pronounced for the rhombus structure. We believe that better overlaps between the *p* orbitals of Al and the C–C π bond in the rhombus structure compared to the linear structure are responsible for the large stabilization effect on the HOMO in the D_{2h} anion.

E. Low-energy electron detachments from the $Al_2C_2^-$ isomers

Since photodetachment involves essentially vertical transitions from the anionic states to that of the neutrals, theoretical VDEs have been found to be valuable to help interpret PES data. As shown above, both isomers of $Al_2C_2^-$ have doublet ground states with the HOMO of the anion singly occupied in both cases (C_{2h} — $1a_g^2 1b_u^2 2a_g^2 2b_u^2 1a_u^2 3b_u^2 3a_g^2 1b_g^1$; D_{2h} — $1a_g^2 1b_u^2 1b_{1u}^2 1b_{2u}^2 2a_g^2 1b_{3u}^2 3a_g^2 2b_{1u}^2 1b_{3g}^1$). Thus, when detaching electrons from the fully occupied MOs, both singlet and triplet excited states of the neutral final states will be produced. However, the current theoretical methods only allow VDEs for the triplet excited states to be calculated. In Tables V and VI, we present the theoretical VDEs, calculated using both UOVGF/6-311+G(2df) and CCSD(T)/6-311+G(2df), for the two isomers of $Al_2C_2^-$. It should be pointed out that the ADEs and VDEs were calculated with a larger basis set (6-311-G(2df)) than that used for the structural optimizations (6-311+G*) given in Tables II–IV. The theoretical results will be used to interpret the experimental PES data in Sec. VI.

VI. INTERPRETATION OF THE PES SPECTRA

A. Features *X′* and *A* and the acetylide isomer

Our calculated VDE for the detachment of the HOMO electron from the acetylide isomer is 0.67 eV at the CCSD(T)/6-311+G(2df) level of theory and 0.65 eV at the UOVGF/6-311+G(2df) level of theory (Table V). The pole strength was found to be 0.91, which indicates that the detachment channel can be primarily described by a one-electron detachment process. The ADE for this detachment channel, i.e., the electron affinity of the neutral Al_2C_2 acetylide, was calculated to be 0.62 eV. These results are in excellent agreement with the measured VDE and ADE for the X' feature (Table I). The relatively sharp nature of the X' feature and the small difference between the VDE and ADE [Fig. 1(a)] are consistent with the fact that there are only very slight geometry changes between the neutral and the anion of the acetylide isomer, as shown in Fig. 2. Therefore, we can assign confidently the X' feature to the acetylide isomer of $Al_2C_2^-$.

The lowest-lying excited state (^3B_g) of the neutral acetylide isomer was calculated to have a VDE of 2.85 eV at the CCSD(T)/6-311+G(2df) level of theory and 3.28 eV at the UOVGF/6-311+G(2df) level of theory (Table V). The results at the two different levels of theory have a relatively large discrepancy of 0.43 eV. As we see above for the X' feature, the CCSD(T)6-311+G(2df) results are in slightly better agreement with the experimental results. If we take the CCSD(T)/6-311+G(2df) result as the VDE for the ^3B_g state, we note that it is in very good agreement with the experimental VDE of the *A* feature (2.91 eV, Table I). The ^3B_g state is due to removal of a nonbonding Al lone pair (Fig. 3,

$3a_g$), and a very sharp peak was expected, in excellent agreement with the sharp nature of the *A* feature. Therefore, we attribute the *A* feature to the ^3B_g excited state of the neutral acetylide isomer. These results suggest a large HOMO–LUMO gap (2.20 eV) for the neutral acetylide.

B. Feature *X* and the planar-bridged isomer

As we see above, the acetylide isomer has a large HOMO–LUMO gap. The strong and broad *X* feature, present in the spectra of all four photon energies (Fig. 1), cannot be associated with the acetylide isomer, and it should be due to another isomer of the $Al_2C_2^-$ anion. Table VI summarizes the theoretical ADE and VDEs for the planar-bridged isomer. Since the rhombus structure of the neutral ground state is a third order saddle point and only the acetylide isomer exists for neutral Al_2C_2 (Tables II and III, Fig. 2), a large geometry change obviously exists between the rhombus anion and the linear neutral. Thus, a very broad band was expected for the detachment of the HOMO electron from the rhombus $Al_2C_2^-$. We note that the measured VDE of 1.58 eV for the *X* band is in good agreement with the calculated VDE of 1.75 (CCSD(T)/6-311+G(2df) or 1.78 eV (UOVGF/6-311+G(2df)) for the rhombus isomer (Table VI). Again, the pole strength was found to be 0.88, indicating that this detachment channel can be primarily described by a one-electron detachment process. The broad nature and the long low energy tail of the *X* band are in excellent agreement with the theoretical predictions. The theoretical ADE of 0.31 eV is also consistent with the long low energy tail, suggesting that the 0–0 transition, that defines the ADE, may have a negligible Franck–Condon factor.

The removal of a β electron from the HOMO-1 ($2b_{1u}^2$, Fig. 4) of the rhombus $Al_2C_2^-$ results in the $^3B_{2u}$ excited state with a calculated VDE of 2.94 eV (Table VI). This predicted VDE agrees well with the *B* feature (Fig. 1), which has an experimental VDE of 3.12 eV. The $2b_{1u}$ MO of the rhombus $Al_2C_2^-$ is a nonbonding orbital, mainly of Al lone pair character with a small contribution from the C–C π bond (Fig. 4). Thus, it is anticipated that the $^3B_{2u}$ excited state of the Al_2C_2 neutral should maintain the rhombus structure with perhaps a slight geometry relaxation. The relatively narrow spectral width of the *B* feature, compared to the *X* feature, is consistent with the nature of the $2b_{1u}$ orbital.

C. Higher binding energy features (*C–H*)

There are numerous higher binding energy features ($C-H$) in the PES spectra in Fig. 1. These features are fairly complicated and should be due to both anionic isomers. As shown in Tables V and VI, there are three additional triplet states due to each anionic isomer in the energy range between 3 and 5.5 eV. We would like to stress that beyond 5.5 eV the one-electron detachment picture of metal containing anions is breaking down according to the recent studies by Dolgounitcheva *et al.*[28] There should also be four singlet excited states, for each isomer, which can also occur in this energy range, but could not be calculated, as mentioned above. The qualitative theoretical picture is consistent with the complicated spectral pattern observed. However, it is not possible to make any definitive assignments for the higher binding energy features, due to limitations of both the current experimental resolution and the accuracy of the theoretical methods. Nevertheless, we are fairly confident that the PES spectral features are due to the two anionic isomers, based on the excellent agreement between the VDEs and spectral widths of the X' and *X* features and the theoretical results. The excellent agreement between the observed large HOMO–LUMO gaps and the theoretical predications provides additional support for the spectral assignments.

VII. DISCUSSION

A. Relative abundance: acetylide versus rhombus $Al_2C_2^-$

On the basis of the relative intensities of the PES features (X' vs *X*), we can infer that the rhombus isomer seemed to be the dominate species in the anion beam. We tried to change the experimental conditions, but could only slightly alter the relative intensities of these two features. Although our current theoretical methods preclude us from firmly concluding which isomer should be the global minimum of the anions, the disparity of the relative intensities of the acetylide and the rhombus isomers was somewhat surprising. Because the acetylide species is the only stable isomer for the neutral Al_2C_2, we would have expected that its corresponding anion should be the dominant one. Interestingly, the disparity in abundance between the two anionic isomers could be understood by considering the formation mechanisms of the clusters. As we showed previously, both AlC_2 and AlC_2^- have π-coordinated structures,[4] from which one can easily conceive that the formation of the rhombus isomer of $Al_2C_2^-$ would be favored. There could be a significant barrier for isomerization from the rhombus isomer to the acetylide structure, although we were unable to calculate this barrier presently.

B. Chemical bonding in X_2C_2: acetylenic versus rhombus structures

It is interesting to consider and compare the chemical bonding and structures of various X_2C_2 species. The structure of the X_2C_2 species is dictated by the nature of the chemical bonding between X and C. When covalent bonding is dominant, a linear acetylene-like structure should be more favorable. For HCCH there have been numerous *ab initio* studies of alternative, nonacetylenic structures.[8,29,30] For example, the vinylidene, bridged-acetylene (nonplanar), and planar-bridged structures have been calculated to be 39.6, 72.1, and 107.1 kcal/mol (all at the MP4/6-31++G**//RHF/6-31++G** level of theory)[29] higher in energy than acetylene, respectively. Among these structures, the planar-bridged structure is actually not a minimum (a second order saddle point) at this level of theory. Schleyer[8] also located the C_s transition state for rearrangement of the bridged-acetylene into vinylidene which was found to be just 0.1 kcal/mol higher in energy at the MP2(full)/6-311G** level of theory. Moreover, the bridged

acetylene lies above the transition state after ZPE correction. Schleyer concluded that bridged-acetylene is not a valuable isomer of acetylene.

When ionic bonding is dominant, the planar-bridged rhombus structure is expected to be more favorable according to simple electrostatic interactions.[7,8] Using the MP2(full)/6-31+G* level of theory, Schleyer[8] analyzed the four structures of Li_2C_2, similar to the HCCH systems mentioned above. He found that both the bridged acetylene and the vinylidene structures collapse to the planar-bridged rhombus structure D_{2h}. Indeed, he found that the rhombus structure is in fact the global minimum with the linear acetylene structure being about 10 kcal/mol higher in energy.

In the current study, we found that the planar-bridged structure for Al_2C_2 is a third order saddle point, the bridged structure (nonplanar) is a second order saddle point, and the vinylidene structure is a first order saddle point. Only the quasilinear structure is a minimum. The vinylidene (slightly nonplanar), bridged acetylene, and planar-bridged structures were found to be 19.1, 23.9, and 24.5 kcal/mol (all at the CCSD(T)/6-311+G*//CCSD(T)/6-311+G* level of theory) higher in energy than the quasilinear structure, respectively. Therefore, we can firmly conclude that there is only one type of minimum for Al_2C_2, corresponding to the quasilinear acetylenic structure (with very small deviation from linearity $<$AlCC=171.3°). The nonlinearity of the acetylenic $Al_2C_2^-$ anion is due to a first order Renner–Teller effect because it has a degenerate electronic state ($^2\Pi_g$) under the $D_{\infty h}$ symmetry.[31] The deviation from a perfect linear structure of the neutral acetylenic Al_2C_2 is attributed to a second order effect due to mixing with low-lying excited states. However we stress that vibrationally averaged structures are essentially linear for both the anion and the neutral species.

To evaluate the ionic and covalent contributions in the Al–C bonds relative to those in the Li–C and H–C bonds, we further performed natural population analyses. Effective atomic charges were calculated for the linear structures: $Q(\mathrm{Li})=+0.92|e|$, $Q(\mathrm{Al})=+0.75|e|$, and $Q(\mathrm{H})=+0.21|e|$. For the planar-bridged structures, we obtained $Q(\mathrm{Li})=+0.87|e|$, $Q(\mathrm{Al})=+0.77|e|$, and $Q(\mathrm{H})=+0.39|e|$. One can see that even though atomic charges are relatively high on Al in both structures, they are smaller than that on Li. Therefore, there is a residual covalent contribution in the Al–C bond that makes the quasilinear structure more favorable. We note that the planar-bridged structure in Al_2C_2 is just 24.5 kcal/mol higher in energy than the linear structure, much smaller than the corresponding quantity of 107.1 kcal/mol found in the H_2C_2 system. In the purely ionic Li_2C_2, the planar-bridged structure becomes the global minimum with the linear structure being about 10 kcal/mol less stable.

In the $Al_2C_2^-$ anion, the highest occupied orbital of the planar-bridged structure is C–C antibonding but Al–C bonding. We believe that the strengthening of the Al–C bond in the anion provides sufficient stabilization, resulting in the planar-bridged structure being a minimum in the anion. As seen in Fig. 2, the Al–C bonds are shortened by almost 0.13 Å in the rhombus anion, relative to the neutral.

C. Relevance to bulk aluminum carbides

The C_2^{2-} unit is a key building block of a large number of binary and ternary metal carbides,[32,33] in particular, in carbides of electropositive elements: alkali, alkali earth, and rare earth. Yet, even though aluminum is a rather electropositive metal, we are not aware of any stable form of Al_2C_2 in the bulk with a C_2^{2-} unit. Instead bulk aluminum carbide has a stoichiometry of Al_4C_3, which reacts with water to produce methane.[32,33] Thus bulk aluminum carbide contains discrete carbon atoms, which can be viewed as C^{4-}, rather than C_2^{2-}. An interesting question is: can a metastable bulk Al_2C_2 be synthesized? To answer this question one needs to study large clusters containing $Al_xC_2(x>2)$ and $(Al_2C_2)_n(n>1)$. We have recently investigated the former and found that the C–C bond is systematically weakened with increasing numbers of Al in Al_xC_2 and will eventually break to form what can be considered to be two C^{4-} units.[34] The $(Al_2C_2)_n$ clusters may be interesting subjects for future investigations in order to further address the question of the possibility to make bulk Al_2C_2.

VIII. CONCLUSIONS

We report a combined experimental and theoretical investigation of Al_2C_2 and its anions. Photoelectron spectra of $Al_2C_2^-$ were measured at various photon energies. Two anionic isomers were identified with numerous detachment transitions. Theoretical calculations were performed for both Al_2C_2 and its anions. Indeed two anionic isomers were found with a quasilinear (acetylide) species and a planar-bridged (rhombus) structure, which are close in energies, whereas only one minimum (quasilinear) was found for the neutral. The energetic information calculated for the two anionic isomers was in excellent agreement with the experimental observations. We found that the acetylide isomer has an electron affinity of 0.64 eV with a large HOMO–LUMO gap. The chemical bonding in Al_2C_2 was compared with that in H_2C_2 and Li_2C_2 and was found to be intermediate between the strong covalent bonding in H_2C_2 and the strong ionic bonding in Li_2C_2. The current study represents the first observation and characterization of the acetylenic Al_2C_2 species.

ACKNOWLEDGMENTS

The theoretical work was done at Utah State University and supported by the donors of The Petroleum Research Fund (Grant No. ACS-PRF# 35255-AC6), administered by the American Chemical Society. The authors thank Professor V. J. Ortiz for valuable discussions of the UOVGF results. The experimental work done at Washington is supported by the National Science Foundation (Grant No. DMR-9622733). The experiment was performed at the W. R. Wiley Environmental Molecular Sciences Laboratory, a national scientific user facility sponsored by DOE's Office of Biological and Environmental Research and located at Pacific Northwest National Laboratory, which is operated for DOE by Battelle under Contract No. DE-AC06-76RLO 1830. L.S.W. is an Alfred P. Sloan Foundation Research Fellow.

[1] X. Li, L. S. Wang, A. I. Boldyrev, and J. Simons, J. Am. Chem. Soc. **121**, 6033 (1999).
[2] A. I. Boldyrev, J. Simons, X. Li, and L. S. Wang, J. Chem. Phys. **111**, 4993 (1999).
[3] L. B. Knight, Jr., S. T. Cobranchi, J. O. Herlong, and C. A. Arrington, J. Chem. Phys. **92**, 5856 (1990).
[4] A. I. Boldyrev, J. Simons, X. Li, and L. S. Wang, J. Am. Chem. Soc. **121**, 10193 (1999).
[5] Y. Apeloig, P. v. R. Schleyer, J. S. Binkley, J. A. Pople, and W. L. Jorgenson, Tetrahedron Lett., 3923 (1976).
[6] J. P. Ritchie and S. M. Bachrach, J. Am. Chem. Soc. **109**, 5909 (1987).
[7] A. Streitwiesser, Jr., Acc. Chem. Res. **17**, 353 (1984).
[8] P. v. R. Schleyer, J. Phys. Chem. **94**, 5560 (1990).
[9] L. S. Wang, H. S. Cheng, and J. Fan, J. Chem. Phys. **102**, 9480 (1998).
[10] L. S. Wang and H. Wu, in *Advances in Metal and Semiconductor Clusters IV*, Cluster Materials, edited by M. A. Duncan (JAI, Greenwich, CT, 1998), pp. 299–343
[11] A. D. McLean and G. S. Chandler, J. Chem. Phys. **72**, 5639 (1980).
[12] T. Clark, J. Chandrasekhar, G. W. Spitznagel, and P. v. R. Schleyer, J. Comput. Chem. **4**, 294 (1983).
[13] M. J. Frisch, J. A. Pople, and J. S. Binkley, J. Chem. Phys. **80**, 3265 (1984).
[14] R. G. Parr and W. Yang, *Density-Functional Theory of Atoms and Molecules* (Oxford University Press, Oxford, 1989).
[15] A. D. Becke, J. Chem. Phys. **96**, 2155 (1992).
[16] J. P. Perdew, J. A. Chevary, S. H. Vosko, K. A. Jackson, M. R. Pederson, D. J. Singh, and C. Fiolhais, Phys. Rev. B **46**, 6671 (1992).
[17] R. Krishnan, J. S. Binkley, R. Seeger, and J. A. Pople, J. Chem. Phys. **72**, 650 (1980).
[18] J. Cizek, Adv. Chem. Phys. **14**, 35 (1969).
[19] G. D. Purvis III and R. J. Bartlett, J. Chem. Phys. **76**, 1910 (1982).
[20] G. E. Scuseria, C. L. Janssen, and H. F. Schaefer III, J. Chem. Phys. **89**, 7382 (1988).
[21] L. S. Cederbaum, J. Phys. B **8**, 290 (1975).
[22] W. von Niessen, J. Shirmer, and L. S. Cederbaum, Comput. Phys. Rep. **1**, 57 (1984).
[23] V. G. Zakrzewski and W. von Niessen, J. Comput. Chem. **14**, 13 (1993).
[24] V. G. Zakrzewski and J. V. Ortiz, Int. J. Quantum Chem. **53**, 583 (1995).
[25] J. V. Ortiz, V. G. Zakrzewski, and O. Dolgunitcheva, in *Conceptual Trends in Quantum Chemistry*, edited by E. S. Kryachko (Kluwer, Dordrecht, 1997), Vol. 3, p. 463.
[26] M. J. Frisch *et al.*, GAUSSIAN 98 (revision A.7), Gaussian, Inc., Pittsburgh, PA, 1998.
[27] MO pictures were made using the MOLDEN3.4 program [G. Schaftenaar, MOLDEN3.4, CAOS/CAMM Center, The Netherlands (1998)].
[28] O. Dolgounitcheva, V. G. Zakrzewski, and J. V. Ortiz, J. Chem. Phys. **111**, 10762 (1999).
[29] J. S. Binkley, J. Am. Chem. Soc. **106**, 603 (1984) and references there.
[30] T. Carrington, Jr., L. M. Hubbard, H. F. Schaefer III, and W. H. Miller, J. Chem. Phys. **80**, 4347 (1984).
[31] G. Herzberg, *Molecular Spectra and Molecular Structure*. III, Electronic Spectra and Electronic Structure of Polyatomic Molecules (Van Nostrand Reinhold Co., New York, 1966).
[32] A. F. Wells, *Structural Inorganic Chemistry*, 5th ed. (Claredon Oxford, 1984).
[33] F. A. Cotton and G. Wilkinson, *Advanced Inorganic Chemistry*, 5th ed. (Wiley, New York, 1988).
[34] L. S. Wang, X. Li, and A. I. Boldyrev (unpublished).